Preeminent Role of the Van Hove Singularity in the Strong-Coupling Analysis of Scanning Tunneling Spectroscopy for Two-Dimensional Cuprate Superconductors

Giorgio Levy de Castro, Christophe Berthod, Alexandre Piriou, Enrico Giannini, and Øystein Fischer

DPMC-MaNEP, Université de Genève, 24 quai Ernest-Ansermet, 1211 Genève 4, Switzerland

(Received 4 April 2007; revised manuscript received 19 March 2008; published 30 December 2008)

In two dimensions the noninteracting density of states displays a van Hove singularity (VHS) which introduces an intrinsic electron-hole asymmetry, absent in three dimensions. We show that due to this VHS the strong-coupling analysis of tunneling spectra in high-T_c superconductors must be reconsidered. Based on a microscopic model which reproduces the experimental data with excellent accuracy, we elucidate the peculiar role played by the VHS in shaping the tunneling spectra, and show that more conventional analysis of strong-coupling effects can lead to severe errors.

DOI: 10.1103/PhysRevLett.101.267004 PACS numbers: 74.72.Hs, 68.37.Ef, 74.25.−q, 74.50.+r

Scanning tunneling spectroscopy of Bi-based cuprate high-T_c superconductors (HTS) shows a d-wave gap and a strong dip-hump feature which is nearly always stronger for occupied than for empty states [1]. It was proposed that the dip-hump structure results from the interaction of electrons with a collective mode [2]. However, such a coupling leads to electron-hole symmetric spectra in classical superconductors [3–5], and the dip asymmetry seen in the cuprates was therefore attributed to the electron-hole asymmetry of the dispersion [6]. The fact that in two dimensions the density of states (DOS) has a prominent van Hove singularity (VHS) introduces naturally an asymmetry. The VHS modifies the strong-coupling analysis and the corresponding determination of the collective mode frequency in an essential way.

Photoemission experiments have provided a detailed account of the band structure in cuprates [7–9]. In agreement with early calculations [10], the band crossing the Fermi level presents a saddle point leading to a logarithmic VHS in the DOS. The scanning tunneling microscope (STM) is the ideal tool to look for such singularities, since under suitable conditions it probes directly the DOS with meV resolution [11–13]. Up to now, however, there was no direct STM observation of the VHS in HTS materials. Previous interpretations of the missing VHS invoked the tunneling matrix element [14,15]: in planar junctions, it is indeed believed that the DOS features in the direction normal to the junction are absent due to a cancellation with the electron velocity, and that the DOS in the plane of the junction does not show up due to focalization effects [16]. These two mechanisms cannot explain the absence of VHS in c-axis STM/HTS tunnel junctions: the Bi-based HTS materials are quasi two-dimensional and have virtually no dispersion in the tunneling direction; the STM junction is qualitatively different from a planar junction and is characterized by a specific matrix element which may not lead to focalization effects [11,12]. Besides, the ability of the STM to probe DOS singularities was recently demonstrated in carbon nanotubes [17].

The solution to this puzzle lies in the coupling to collective modes. It is known that this coupling induces the dip feature [6,18] and suppresses the VHS peak in the DOS [19]. Here we demonstrate that the interplay of the VHS with the collective mode provides a complete explanation of both the missing VHS and the pronounced electron-hole asymmetries.

We studied the three-layer compound $Bi_2Sr_2Ca_2Cu_3O_{10+\delta}$ (Bi2223), which has the highest T_c and the most pronounced dip feature in the Bi-based family. Our single crystals cleaved *in situ* in UHV at room temperature yield reproducible spectroscopy [20]. The tunneling conductance measured on an optimally-doped sample is shown in Fig. 1. The spectrum presents the characteristic low-energy conductance of d-wave superconductors, strong and asymmetric coherence peaks, and an electron-hole asymmetric dip-hump structure. We have deliberately selected an optimally-doped sample displaying a flat background conductance at high energies (inset of Fig. 1). For underdoped samples the spectra present an asymmetric background, attributed to strong correlation effects [21–23]. By selecting a sufficiently doped sample we stay away from this regime. We can therefore exclude that the asymmetries observed in Fig. 1 result from this type of correlations, since the background is absent.

For illustrative purposes, we plot in Fig. 1 the prediction of a conventional free-electrons BCS d-wave model [24,25]. This model fits the experimental data well at low energy, but fails to account for the various features present at higher energy. A better description of the asymmetric coherence peaks can be achieved by taking into account the actual band structure. We consider the two-dimensional lattice model $\xi_{\boldsymbol{k}} = 2t_1(\cos k_x + \cos k_y) + 4t_2 \cos k_x \cos k_y + 2t_3(\cos 2k_x + \cos 2k_y) - \mu$, where t_i is the ith neighbor hopping energy [26]. For this dispersion the VHS lies at

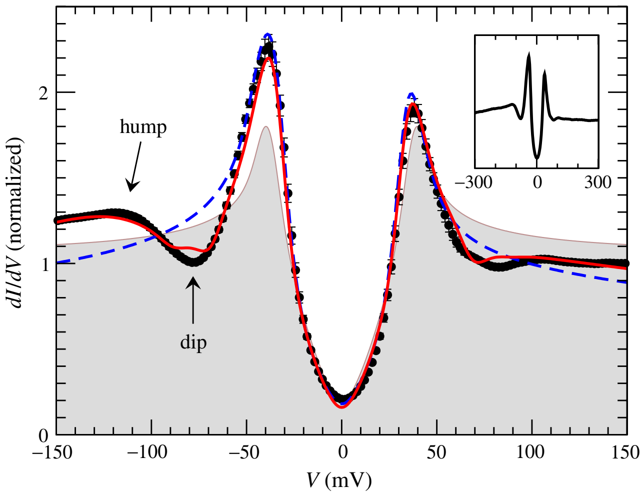

FIG. 1 (color online). Typical STM conductance of Bi2223 ($T_c = 111$ K) at $T = 2$ K (dots). The data are an average of 15 spectra taken at different positions on the same sample, and having the same peak-to-peak gap $\Delta_p = 38$ meV. Error bars give the standard deviation of this average. The inset shows the spectrum on a larger energy scale. Also shown are three model predictions (see text): free-electrons d-wave BCS (shaded area), d-wave BCS with realistic dispersion including VHS (dashed line), and d-wave BCS including VHS and coupling to the collective mode (full line). The total spectral weight in the energy range of the figure is the same for all curves.

an energy $\xi_M = -4(t_2 - t_3) - \mu$. We determine the parameters of the band by fitting the whole spectrum in the inset of Fig. 1, which leads to $t_1 = -882$, $t_2 = 239$, $t_3 = -14$, and $\xi_M = -26$ meV, as well as a d-wave gap $\Delta_0 = 34.1$ meV. It is remarkable that these band parameters extracted directly from the STM conductance lead to a Fermi surface in semiquantitative agreement with the one measured by photoemission [8,27]. The resulting theoretical curve (Fig. 1, dashed line) is very similar to the free-electron model at subgap energies, but follows more closely the experiment up to an energy slightly outside the coherence peaks. The main effect of the VHS is to provide additional spectral weight below the Fermi level and thus to increase the height of the coherence peaks at negative bias.

The "BCS plus VHS" model is not satisfactory above $eV \sim 2\Delta_p$, where it fails to reproduce the significant transfer of spectral weight from the dip to the hump, which is strongest at negative bias in the experimental spectrum. Generically, such transfers signal a strong interaction of the quasiparticles with a collective excitation, which leads to enhanced damping of the former. In conventional superconductors the electron-phonon coupling is known to induce similar features, albeit much less pronounced, at biases related to the phonon frequencies [3–5]. Several authors have recently proposed that the dip-hump in HTS is due to phonons [28–33]. Another candidate is the (π, π) magnetic excitation [2,6,18] known as the "41 meV resonance" [34]. Coupling the quasiparticles to this collective mode leads to a change of the electron self-energy which can be expressed in terms of the spin susceptibility $\chi_s(\boldsymbol{q}, \omega)$ [6]. Using a parametrization of χ_s as measured by inelastic neutron scattering, Hoogenboom *et al.* showed that this model provides a very good description of the STM spectra of Bi2212 at several dopings [19]. Apart from the band-structure parameters t_i, μ and the d-wave gap Δ_0, this model has 3 more parameters, namely, the resonance energy Ω_s, a characteristic length $\xi_s \sim 2a$ which describes the spread of the collective mode around $\boldsymbol{q} = (\pi, \pi)$, and a coupling constant g [6].

In order to estimate these parameters we again perform a least-squares fit of the whole spectrum shown in the inset of Fig. 1, keeping the t_i's fixed to their values determined previously. This procedure yields $\Delta_0 = 33.9$ meV, $\xi_M = -42.4$ meV, and $\Omega_s = 34.4$ meV, in reasonable agreement with the properties of the magnetic resonance measured in Bi2223 [35]. The resulting theoretical spectrum matches our experimental data with excellent accuracy (Fig. 1, full line). In particular, the model reproduces all of the asymmetries found experimentally between positive and negative biases. We would like to stress that these asymmetries cannot be explained by models which neglect the band structure [32,36]. The shape of the dip minimum in the theoretical curve differs from experiment: we shall come back to this below. Fits of similar quality have been obtained for many different spectra with gaps varying from $\Delta_p = 36$ to 54 meV.

The precise interpretation of the theoretical curve in Fig. 1 is complicated due to the interplay of three similar energy scales: the d-wave gap Δ_0, the VHS energy ξ_M, and the collective mode energy Ω_s, all in the 30–40 meV range. After a careful study of the model we can identify the origin of each feature in the spectrum, as illustrated in Fig. 2. The bare BCS DOS $N_0(\omega)$ exhibits 5 singularities: namely, (a) the V at zero energy resulting from the d-wave gap; (b) and (b') the coherence peaks at negative and positive energies ($-\omega_b$ and $\omega_{b'}$ respectively); (c) the VHS at energy $-\omega_c$ below the coherence peak, and (c') the weak echo of the VHS at energy $\omega_{c'}$ due to the BCS electron-hole mixing. The interaction with a collective mode leads to inelastic processes in which a quasiparticle of momentum $\boldsymbol{k}$ and energy ω is scattered to a state with momentum $\boldsymbol{k} - \boldsymbol{q}$ and energy $\omega - \Omega$ through emission of a collective excitation with quantum numbers $(\boldsymbol{q}, \Omega)$. The corresponding self-energy diagram is sketched in Fig. 2. If the only excitation available is a sharp-in-energy mode, all singularities of $N_0(\omega)$ are mirrored in the self-energy, and exactly shifted by the mode energy Ω_s. Hence the DOS $N(\omega)$ including the interaction with the mode displays 3 pairs of singularities indicated by arrows in Fig. 2: the onsets at $\omega = \pm\Omega_s$, below which the quasiparticles do not have enough energy to excite a collective mode, a first minimum in the dip at $-\omega_b - \Omega_s$ (respectively, $\omega_{b'} + \Omega_s$) corresponding to the negative-energy (positive-energy) coherence peak, and a second minimum in the dip—echoing

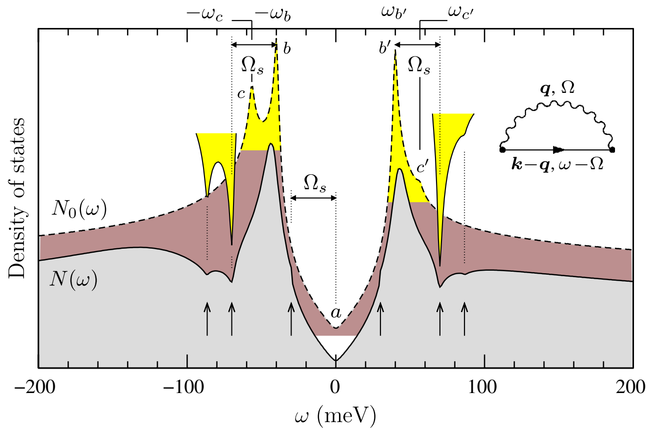

FIG. 2 (color online). High-resolution calculation of the DOS in the absence [$N_0(\omega)$, dashed line, shifted vertically] and in the presence [$N(\omega)$, full line] of the coupling to the (π, π) resonance. The energy and shape of the structures induced by this coupling (arrows) is an "inverted image" of the singularities present in the BCS DOS (a, b, b', c, c'), shifted by the mode energy Ω_s. The parameters are as in Fig. 1, except for $\Delta_0 = 40$, $\xi_M = -40$, and $\Omega_s = 30$ meV. The inset shows the self-energy diagram with the full line representing the BCS Green's function and the wavy line the spin susceptibility.

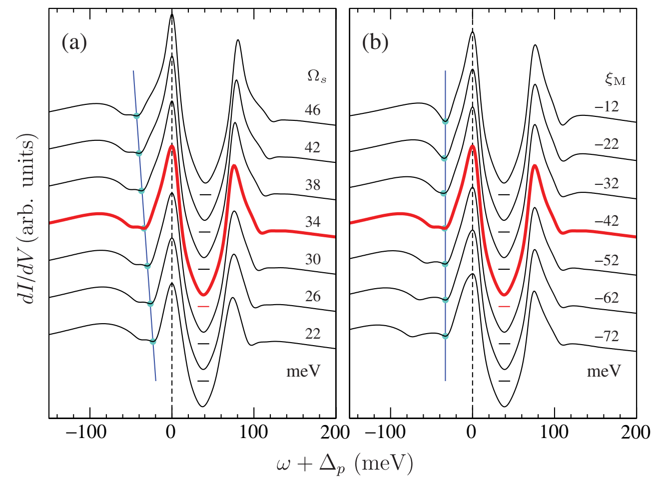

FIG. 3 (color online). Evolution of the theoretical tunneling conductance upon varying Ω_s (a) or ξ_M (b). The other model parameters are as in Fig. 1. Energies are measured relative to the peak maximum at $-\Delta_p$. The values of Ω_s and ξ_M span a larger range than their possible variation in the experiment (Fig. 4), but were chosen so with the aim of amplifying the trends.

the VHS peak in $N_0(\omega)$—which is more pronounced for occupied states at $-\omega_c - \Omega_s$, but also visible at $\omega_{c'} + \Omega_s$. Therefore the asymmetry of the dip structure between positive and negative biases receives a natural explanation in terms of the asymmetry of the underlying BCS DOS, which in turn is due to the VHS. The appearance of a double minimum in the dip is a direct consequence of the BCS DOS having both a coherence peak at $-\omega_b$ and a VHS peak at $-\omega_c$. Such a double minimum is not observed in the experimental spectrum of Fig. 1. It is also not seen on SIS spectra which generally present sharper structures [18,36]. At positive bias, the various broadening effects [25] are sufficient to smear out the two minima into one. On the other hand, we have found that if the collective mode has a finite inverse lifetime of only ~6 meV [35], then the two minima in the dip fade away resulting in a smooth dip also at negative bias as observed experimentally.

The exact relationship between the position of the various structures in $N(\omega)$ and the parameters of the model is not straightforward. The first minimum in the dip at negative energy lies to a good approximation at $-\Delta_p - \Omega_s$, and the second at $-(\xi_M^2 + \Delta_p^2)^{1/2} - \Omega_s$. In Fig. 3 we illustrate these two dependencies by varying Ω_s and ξ_M independently in the model. Our starting point is the spectrum of Fig. 1 reproduced in bold in Fig. 3. Varying Ω_s while keeping ξ_M fixed we see that the main change in the spectrum is a displacement of the dip and hump with respect to the peak, consistently with the interpretation given in Fig. 2. In particular, the width of the dip at negative bias does not depend on Ω_s. As Ω_s increases, we also observe that the coherence peaks become taller and develop a shoulder. This shoulder carries part of the spectral weight expelled from the dip, and progressively exits the coherence peak as Ω_s increases. Figure 3(a) further shows that Ω_s has not much influence on the electron-hole asymmetry of the spectra. In contrast, changing the position of the VHS by varying ξ_M dramatically affects this asymmetry. At the lowest ξ_M considered the spectrum is almost symmetric. As the VHS moves toward negative energy, the dip at $\omega < 0$ gets wider (the first minimum in the dip does not move, as expected) and the dip at $\omega > 0$ vanishes. Inspection of Fig. 3 also shows that the maximum of the hump feature tracks the second minimum in the dip, and thus depends on both Ω_s and ξ_M. Furthermore, the hump gets flattened as $|\xi_M|$ increases.

The trends identified in Fig. 3 by varying independently the model parameters Ω_s and ξ_M can now be used to interpret the experimental spectra. In Fig. 4 we plot a series of tunneling conductance spectra with peak-to-peak gaps ranging from $\Delta_p = 36$ to 54 meV. These spectra were defined with the procedure outlined in the caption of Fig. 1 from raw data recorded at different locations on the same surface. The evolution of the spectra with Δ_p is also consistent with data obtained on many samples. As Δ_p increases, we first observe that (i) the dip for occupied states gets wider, (ii) the dip for empty states gets weaker, and (iii) the hump at negative energy flattens out. These three trends are observed in Fig. 3(b), strongly suggesting that the increase of Δ_p is accompanied by a shift of the VHS towards negative energies. This is also consistent with the idea that local increases of Δ_p in inhomogeneous samples reflect local decreases in the hole concentration. Another obvious trend of the data in Fig. 4 is that the coherence peaks are reduced with increasing gap [37]. As seen in Fig. 3(b), this is also consistent with a shift of

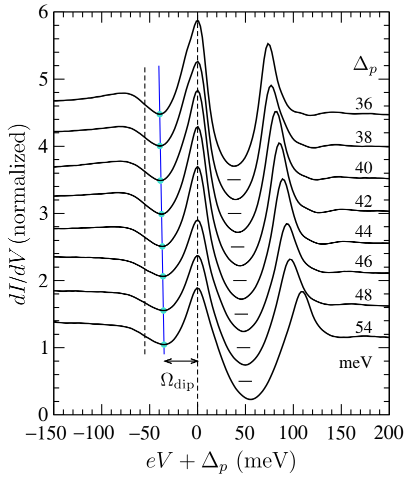

FIG. 4 (color online). STM conductance spectra of Bi2223 ($T_c = 111$ K) at $T = 2$ K. Each curve is an average of several spectra taken at different locations on the same sample, all having the indicated peak-to-peak gap Δ_p. $\Omega_{\rm dip}$ is the energy difference between the dip minimum (dot) and the peak maximum at negative bias, relative to which voltages are measured.

the VHS to lower energy. However, a look at Fig. 3(a) shows that this trend can also be ascribed to a decrease in the value of Ω_s. Our calculations indeed confirm that Ω_s, as determined by fits to the spectra in Fig. 4, decreases from 34 to 24 meV with increasing Δ_p. The energy difference between the coherence peak and the dip minimum in the experimental spectra, $\Omega_{\rm dip}$, also decreases with increasing Δ_p, but less than Ω_s (from 39 to 35 meV). From these numbers it appears clearly that $\Omega_{\rm dip}$ overestimates Ω_s by 5 to 10 meV. Recently the energy difference between Δ_p and the inflection point between the dip and the hump (minimum in the d^2I/dV^2 spectrum) was used as an estimate of Ω_s in Bi2212 [31], resulting in an average value of 52 meV. This same estimate would give a Δ_p-independent result of $\sim$57 meV for the data in Fig. 4 (dashed line), almost a factor of 2 larger than Ω_s.

In summary, we have shown that the van Hove singularity plays a crucial role in the shape and electron-hole asymmetry of the spectral features induced in the DOS by the interaction of quasiparticles with a collective mode. As a result, the determination of the mode energy directly from STM data is complicated, and cannot generally be done by looking for structures in the dI/dV or d^2I/dV^2 spectra. Although in the present study we focused on Bi2223, our conclusions are relevant to Bi2212, and more generally to all quasi-2D materials displaying electron-hole asymmetry. A systematic application of our methodology to various layered cuprates promise to give valuable information about the spin resonance, and its role in high-T_c superconductivity.

We thank I. Maggio-Aprile and Y. Fasano for useful discussions. This work was supported by the Swiss National Science Foundation through Division II and MaNEP.

[1] C. Renner and Ø. Fischer, Phys. Rev. B **51**, 9208 (1995).
[2] J.C. Campuzano *et al.*, Phys. Rev. Lett. **83**, 3709 (1999).
[3] G.M. Eliashberg, Sov. Phys. JETP **11**, 696 (1960).
[4] I. Giaever *et al.*, Phys. Rev. **126**, 941 (1962).
[5] W.L. McMillan and J.M. Rowell, Phys. Rev. Lett. **14**, 108 (1965).
[6] M. Eschrig and M.R. Norman, Phys. Rev. Lett. **85**, 3261 (2000).
[7] A. Damascelli *et al.*, Rev. Mod. Phys. **75**, 473 (2003).
[8] D.L. Feng *et al.*, Phys. Rev. Lett. **88**, 107001 (2002).
[9] T. Sato *et al.*, Phys. Rev. Lett. **91**, 157003 (2003).
[10] W.E. Pickett, Rev. Mod. Phys. **61**, 433 (1989).
[11] J. Tersoff and D.R. Hamann, Phys. Rev. Lett. **50**, 1998 (1983).
[12] C.J. Chen, Phys. Rev. Lett. **65**, 448 (1990).
[13] Ø. Fischer *et al.*, Rev. Mod. Phys. **79**, 353 (2007).
[14] K. Kouznetsov and L. Coffey, Phys. Rev. B **54**, 3617 (1996).
[15] Z. Yusof *et al.*, Phys. Rev. B **58**, 514 (1998).
[16] W.A. Harrison, Phys. Rev. **123**, 85 (1961).
[17] M. Ouyang *et al.*, Science **292**, 702 (2001).
[18] J.F. Zasadzinski *et al.*, Phys. Rev. Lett. **87**, 067005 (2001).
[19] B.W. Hoogenboom *et al.*, Phys. Rev. B **67**, 224502 (2003).
[20] M. Kugler *et al.*, J. Phys. Chem. Solids **67**, 353 (2006).
[21] W. Rantner and X.-G. Wen, Phys. Rev. Lett. **85**, 3692 (2000).
[22] P.W. Anderson and N.P. Ong, J. Phys. Chem. Solids **67**, 1 (2006).
[23] M. Randeria *et al.*, Phys. Rev. Lett. **95**, 137001 (2005).
[24] H. Won and K. Maki, Phys. Rev. B **49**, 1397 (1994).
[25] Our theoretical curves in Figs. 1 and 3 show the DOS corrected by three broadening effects: a constant scattering rate $\Gamma = 2$ meV, a 2 K thermal smearing, and a Gaussian broadening of 4 meV. The latter accounts for the combined experimental uncertainty due to the lock-in ac modulation at $V_{\rm ac} = 2$ mV, and the averaging of several slightly different spectra.
[26] Multilayer effects are neglected. It was shown in Ref. [19] that in Bi2212 the structures related to the bonding band are largely suppressed by self-energy effects.
[27] We consider our band parameters as an effective model for the low-energy dispersion: these parameters are not expected to describe the experimental dispersion above 300 meV, and, in particular, the total bandwidth.
[28] A.W. Sandvik *et al.*, Phys. Rev. B **69**, 094523 (2004).
[29] T.P. Devereaux *et al.*, Phys. Rev. Lett. **93**, 117004 (2004).
[30] R. Citro *et al.*, Phys. Rev. B **73**, 014527 (2006).
[31] J. Lee *et al.*, Nature (London) **442**, 546 (2006).
[32] S. Pilgram *et al.*, Phys. Rev. Lett. **97**, 117003 (2006).
[33] G. Zhao, Phys. Rev. B **75**, 214507 (2007).
[34] Y. Sidis *et al.*, Phys. Status Solidi B **241**, 1204 (2004).
[35] In a $T_c = 110$ K Bi2223 sample, the (π, π) resonance was observed by neutron scattering at $\Omega_s = 42$ meV with intrinsic energy and momentum widths of 12 meV and 0.37 Å^{-1}, respectively. S. Pailhès (private communication).
[36] J.F. Zasadzinski *et al.*, Phys. Rev. Lett. **96**, 017004 (2006).
[37] We also observe that the coherence peaks become more symmetric with increasing gap.